

# FANCD2 and REV1 cooperate in the protection of nascent DNA strands in response to replication stress

Yeran Yang<sup>1,†</sup>, Zhenbo Liu<sup>1,†</sup>, Fengli Wang<sup>2,†</sup>, Piya Temviriyankul<sup>3</sup>, Xiaolu Ma<sup>1</sup>, Yingfeng Tu<sup>2</sup>, Lingna Lv<sup>1</sup>, Yu-Fen Lin<sup>4</sup>, Min Huang<sup>1</sup>, Ting Zhang<sup>1</sup>, Huadong Pei<sup>5</sup>, Benjamin P.C. Chen<sup>4</sup>, Jacob G. Jansen<sup>3</sup>, Niels de Wind<sup>3</sup>, Paula L. Fischhaber<sup>6</sup>, Errol C. Friedberg<sup>7</sup>, Tie-Shan Tang<sup>2,\*</sup> and Caixia Guo<sup>1,\*</sup>

<sup>1</sup>Key Laboratory of Genomics and Precision Medicine, China Gastrointestinal Cancer Research Center, Beijing Institute of Genomics, Chinese Academy of Sciences, Beijing 100101, China, <sup>2</sup>State Key Laboratory of Membrane Biology, Institute of Zoology, Chinese Academy of Sciences, Beijing 100101, China, <sup>3</sup>Department of Human Genetics, Leiden University Medical Center, 2300 RC, Leiden, The Netherlands, <sup>4</sup>Department of Radiation Oncology, UT Southwestern Medical Center, Dallas, TX 75390, USA, <sup>5</sup>Beijing Proteome Research Center, Beijing Institute of Radiation Medicine, Beijing 102206, China, <sup>6</sup>Department of Chemistry and Biochemistry, California State University Northridge, Northridge, CA 91330-8262, USA and <sup>7</sup>Department of Pathology, UT Southwestern Medical Center, Dallas, TX 75390, USA

Received January 02, 2015; Revised July 06, 2015; Accepted July 08, 2015

## ABSTRACT

**REV1 is a eukaryotic member of the Y-family of DNA polymerases involved in translesion DNA synthesis and genome mutagenesis. Recently, REV1 is also found to function in homologous recombination. However, it remains unclear how REV1 is recruited to the sites where homologous recombination is processed. Here, we report that loss of mammalian REV1 results in a specific defect in replication-associated gene conversion. We found that REV1 is targeted to laser-induced DNA damage stripes in a manner dependent on its ubiquitin-binding motifs, on RAD18, and on monoubiquitinated FANCD2 (FANCD2-mUb) that associates with REV1. Expression of a FANCD2-Ub chimeric protein in RAD18-depleted cells enhances REV1 assembly at laser-damaged sites, suggesting that FANCD2-mUb functions downstream of RAD18 to recruit REV1 to DNA breaks. Consistent with this suggestion we found that REV1 and FANCD2 are epistatic with respect to sensitivity to the double-strand break-inducer camptothecin. REV1 enrichment at DNA damage stripes also partially depends on BRCA1 and BRCA2, components of the FANCD2/BRCA supercomplex. Intriguingly, analogous to FANCD2-mUb and BRCA1/BRCA2, REV1 plays an unexpected role in protecting nascent repli-**

**cation tracts from degradation by stabilizing RAD51 filaments. Collectively these data suggest that REV1 plays multiple roles at stalled replication forks in response to replication stress.**

## INTRODUCTION

REV1 is a member of the translesion DNA synthesis (TLS) family of specialized DNA polymerases and is responsible for the majority of spontaneous and DNA damage-induced mutagenesis *in vivo* (1–3). REV1 co-localizes with proliferating cell nuclear antigen (PCNA) in replication factories (4) and binds with monoubiquitinated PCNA in cells exposed to UV radiation (5). REV1 is believed to function as a scaffold protein for polymerase switching at sites of lesions during TLS (6). Recent studies indicate that the Fanconi anemia (FA) core complex controls REV1-mediated TLS after UV radiation in a FANCD2-independent fashion (7–9). In addition, the breast cancer-associated protein BRCA1, which interacts with REV1 and E3 ubiquitin ligase RAD18, also regulate REV1-mediated TLS after UV radiation (10).

Beyond its primary role in TLS, REV1 can localize at regions near double-strand breaks (DSBs) in budding yeast (11). DSBs initiate diverse responses, including homologous recombination (HR), which in eukaryotes mainly results in gene conversion. This process involves the unidirectional transfer of genetic material from a donor sequence to a homologous acceptor sequence. Gene conversion may

\*To whom correspondence should be addressed. Tel: +86 10 84097646; Fax: +86 10 84097720; Email: guocx@big.ac.cn  
Correspondence may also be addressed to Tie-Shan Tang. Tel: +86 10 64807296; Fax: +86 10 64807296; Email: tangtsh@ioz.ac.cn  
†These authors contributed equally to the paper as first authors.

also result from template switching by replisomes stalled at replication-blocking DNA lesions, or difficult-to-replicate DNA structures. Template switching during HR involves strand invasion mediated by filaments of the single strand DNA binding protein RAD51. Recently it has been reported that REV1 is involved in HR in chicken DT40 cells (12), *Drosophila melanogaster* (13) and human cells (14). However, it remains unclear how REV1 is recruited to sites where HR is processed.

Although FANCD2 is not required for UV-induced REV1 foci formation and associated mutagenesis (8), it colocalizes with REV1 following treatment with agents that strongly induce HR, such as hydroxyurea (HU) and thymidine (15), hinting that FANCD2 might regulate REV1 recruitment to sites where HR is processed. Additionally, considering that RAD18 can target to DSBs and is essential for appropriate activation of the FA pathway after treatment with the Topoisomerase 1 inhibitor camptothecin (CPT) (16,17), a compound that induces replication-coupled DSBs during S phase (17), we speculate that RAD18 regulates REV1 recruitment to HR processing sites, despite the fact that the RAD18-dependent DSB repair pathway is not related to monoubiquitinated PCNA (17).

In this study, we first reveal a role of the BRCA1 C-terminal (BRCT) domain of REV1 in replication-associated gene conversion, using a genomic reporter construct. Then we reveal the involvement of RAD18 and the ubiquitin-binding motifs (UBMs) of REV1, monoubiquitinated FANCD2 (FANCD2-mUb), BRCA1 and BRCA2 in the recruitment of REV1 to UVA laser-induced double-stranded DNA breaks. Additionally, REV1 and FANCD2 display epistasis with respect to sensitivity to CPT. Finally, using a DNA fiber resection assay, we reveal that REV1 protects nascent replication tracts following exposure to CPT and HU. Our results indicate that REV1 plays multiple roles at stalled replication forks to maintain genomic integrity in response to replication stress.

## MATERIALS AND METHODS

### Plasmids and reagents

To generate the HisD reporter plasmid, a PCR fragment containing the complete 1.3 kb coding sequence of HisD was amplified using primers 5'-GGCCCGGGACCA TGGGCTCAATACCCTGAT TGAC-3' and 5'-CCGA ATTCCTAGGTCATGCTTGCTCCTTGAGGG-3'. This fragment was cloned into the plasmid pVito-blasti-mcs (Invivogen) downstream of the rEF1 promoter that drives transcription of the *Bsr* gene conferring resistance to blasticidin (Bsd). The HisD coding sequence was interrupted upon introduction of two SalI sites in tandem into a unique BspEI site in the 3' part of the gene (HisD\*). An IRES sequence allows expression of *Bsr*. A 428 bp PCR fragment containing the 3' part of HisD was generated using primers 5'-CCGAATTCAG GCCCTGAGCGCCAG TC-3' and 5'-CCGAATTCCTAGGTCATGCTTGCTCCTTGAGGG-3'. This 3' HisD fragment was cloned downstream of the *Bsr* gene and acts as donor sequence to enable restoration of the HisD\* allele to a functional HisD gene.

For binding assays, mouse *Rev1* cDNA was cloned in pEGFP-C3 (Clontech) or p3xFlag-CMV (Sigma) to gen-

erate eGFP or Flag fusion proteins. The pSFB-FANCD2 K561R plasmid encoding a FANCD2 protein with a K561R mutation was a gift from Dr Larry M Karnitz (Mayo Clinic College of Medicine). The ubiquitin cDNA lacking the C-terminal Gly-Gly codons was cloned to pSFB-FANCD2 K561R plasmid to make a full-length FANCD2-ubiquitin chimera (FancD2-Ub) as described previously (18). The construct with mutations in mREV1 UBMs and GFP-RAD51 were generated as described previously (5,19). The pSFB-FANCI plasmid was a gift from Dr Junjie Chen (UT MD Anderson Cancer Center).

Anti-Flag M2 agarose affinity gel and mouse monoclonal antibody against  $\beta$ -actin (clone AC15) or Flag were purchased from Sigma (St Louis, MO, USA). Antibody against  $\gamma$ H2AX was from the Cell Signalling Technology (Danvers, MA, USA). Antibody against FANCD2 (FI17) was from Santa Cruz Biotechnology. Antibodies against HA, Myc and GFP were from Covance. Antibodies against KU80 and  $\beta$ -TUBULIN were from Beijing Protein Innovation (Beijing, China). Alexa Fluor-conjugated secondary antibodies were from Invitrogen. Rabbit polyclonal antiserum against REV1<sup>872-1150</sup> was made by Covance.

### Cell culture and reagents

Human HCT116, U2OS and 293T cells were obtained from the American Type Culture Collection (Rockville, MD, USA). FANCD2-deficient PD20 cells were obtained from the Fanconi Anemia Research Fund (20). All cell lines were grown in DMEM medium supplemented with 10% fetal bovine serum at 37°C in the presence of 5% CO<sub>2</sub> if not specified. For transient transfection experiments, cells were transfected with indicated constructs, using Fugene 6 (Roche) or Lipofectamin 2000 (Invitrogen) following the manufacturer's protocols.

### RNA interference

The introduction of small interfering RNA (siRNA) into cells was carried out with RNAiMAX (Invitrogen). For REV1 recruitment study, cells were further transfected with GFP-REV1 using Lipofectamin 2000 (Invitrogen) at 48 h after siRNA transfection. About 40 h later, the cells were micro-irradiated and processed for immunofluorescence as described below. Whole cell lysates were harvested at 72 h after siRNA transfection.

siRNAs directed against human *FANCD2*, *REV1*, *BRCA1* or *BRCA2* were obtained from GenePharma (Shanghai, China). The gene-specific target sequences were as follows: *FANCD2-1* (UUGGAGGAGAU-GAUGGUCUA) (7), *FANCD2-2* (CUAGCACCGUAU-UCAAGUA), *FANCD2-3* (CGAGUUGUGGCAU-UGUU), *FANCD2-4* (CAACAUACCUCGACUCAU), *REV1-1* (GAACAGUGACGCAGGAAUA) (21), *REV1-2* (AAGCAUCAAGCUGGACGACU) (22), *BRCA1* (UAUAAGACCUCUGGCAUGAAU), *BRCA2* (AA-CAACAAUACGAACCAAACUU) (23). The negative control siNC sequence (UUCUCCGAACGUGU-CACGU) was obtained from GenePharma. Unless otherwise specified, *REV1-1* and *FANCD2-1* were used as the representative siRNA against *REV1* and *FANCD2*

in all human cell experiments, respectively. The gene-specific target sequences against mouse *Fancd2* were as follows: *mFancd2-1* (GCUAGAUUCUGAGGAUAAA), and *mFancd2-2* (GAGGAAGCAUCCUGCUUUAU). The mixture of *mFancd2-1* and *mFancd2-2* was used to knock down FANCD2 expression in mouse cells. The gene-specific target sequences against mouse *Mre11* were as follows: *mMre11-1* (GCUGCUUGGAGCUGCUUAG), and *mMre11-2* (ACAGGAGAAGAGAUC AACU). The mixture of *mMre11-1* and *mMre11-2* was used to knock down Mre11 expression in mouse cells. Western blots were used to validate the extent of knockdown by these siRNAs.

#### Establishment of FANCD2 and REV1 stable knockdown cells

The human shRNA-*FANCD2* plasmids (TRCN0000082840 and TRCN0000082842), shRNA-*REV1* plasmid (TRCN0000152109) and a non-targeting control plasmid (shRNA-SHC002) were purchased from Open Biosystems. Stable FANCD2 knockdown or negative control clones were generated by infecting U2OS cells with polybrene-supplemented medium obtained from 293T packaging cells transfected with the shRNA-*FANCD2* or shRNA-SHC002. Individual clones were isolated by limiting dilution in media containing puromycin and screened for FANCD2 expression levels with antibodies against FANCD2. Stable REV1 knockdown or negative control cells were generated by infecting 293T cells with polybrene-supplemented medium obtained from 293T packaging cells transfected with the human shRNA-*REV1* plasmid or shRNA-SHC002 (shNC). Puromycin-resistant stable cells were selected for HR assay.

#### Laser microirradiation and imaging

The microirradiation was carried with a pulsed nitrogen laser (365 nm, 10 Hz pulse) as previously described (24,25). Briefly, cells were seeded on 35-mm glass bottom dishes (MatTek) overnight before being visualized with a Nikon Eclipse Ti-E inverted microscope equipped with a computer-controlled MicroPoint laser Ablation System (Photonics Instruments). The output of laser power was set to five pulses and 30–40% of transmission which was the lowest power that reproducibly gave a focused  $\gamma$ H2AX stripe. For quantitating the percentage of cells with REV1 accumulation at sites of laser irradiation, GFP-REV1 expressing cells were selected for laser microirradiation. The frequency of cells which exhibit a visible accumulation of REV1 along the line of irradiation at 10 min after microirradiation was determined. Standard errors were derived from at least three independent experiments. To further compare, the amount of GFP-REV1 at damage sites at certain time points, we have used a computer-aided analysis system to quantify the amount of the accumulated GFP-REV1 as described previously (24,26). Briefly, we used MetaMorph (Version 7.7.5.0) to measure the grey value of each irradiated site in cells to represent the amount of accumulated GFP-REV1. Then the average fluorescence intensity (gray level) of GFP-REV1 was calculated and compared. To be specific, the microirradiation sites were marked as ROIs (region of interest), and the grey values of these ROIs were

measured under the 'Region Measurements' function. The grey value in undamaged region was subtracted from that of ROIs for each cell at each time point to determine the final value reported. The associated standard errors were derived from 10 independent measurements.

#### Immunofluorescence

Cells were fixed in 4% paraformaldehyde for 10 min at room temperature, and then permeabilized with 0.5% Triton X-100 for 15 min. The permeabilized cells were blocked with 5% fetal bovine serum/ 0.1% Tween 20 for 60 min at room temperature and incubated with primary antibodies against  $\gamma$ H2AX at room temperature for 45 min. Cells were then incubated with the appropriate Alexa Fluor dye conjugated secondary antibody (Molecular Probes) for 45 min. The cells were further counterstained with DAPI to visualize nuclear DNA. Images were taken with equal exposure time. For quantitative analysis of UV-induced REV1 focus formation, U2OS cells transfected with GFP-REV1 were treated with UVC (15 J/m<sup>2</sup>) and fixed with 4% paraformaldehyde 12 h later after UV irradiation as described previously (27). Images were acquired with a Leica DM5000 (Leica) equipped with HCX PL S-APO 63 $\times$ 1.3 oil CS immersion objective (Leica) and processed with Adobe Photoshop 7.0.

#### Coimmunoprecipitation and Western blotting

HEK293T cells transfected with pCMV-HA-mREV1 and pSFB-FANCD2 K561R-2 (pSFB-FANCD2\*) or pSFB-FANCD2-Ub were harvested and immunoprecipitation with anti-Flag M2 agarose in the presence of the DNA intercalator ethidium bromide (EtBr) was performed using whole cell lysates as described previously (28). A similar immunoprecipitation was performed using HEK293T cells transfected with Flag-mREV1 and GFP-RAD51. HEK293T cells transfected with pCMV-HA-mREV1 were treated with CPT (5  $\mu$ M) for 2 h and crosslinked with 10 mM Dimethyl 3,3-dithiobispropionimidate 2 HCl (DTBP) in PBS for 40 min at 4°C. The reaction was stopped by a 5-min incubation with 1 M Tris-Cl (pH 8.0). Then the whole cell lysates were immunoprecipitated with anti-FANCD2 antibody. Samples were separated by SDS-PAGE and detected by immunoblotting with indicated antibodies.

#### Chromatin immunoprecipitation

DR-GFP HeLa cells with one copy of the DR-GFP gene stably integrated into its genome (29) were transfected with either WT or UBM\* pCMV-HA-REV1 (5). After I-*SceI* induction of DSBs, chromatin was immunoprecipitated from the cells using antibodies against either  $\gamma$ H2AX or HA and quantitative polymerase chain reaction (qPCR) was used to determine REV1 recruitment to the induced break sites as previously described (29). Input DNA was used as an internal control for each qPCR to normalize the CHIP signal. For all CHIP experiments data are shown as mean $\pm$ SEM of three independent CHIP experiments.

### HisD reversion assay

Immortalized *Rev1* WT, *Brc1* mutant (containing a defined deletion in the N-terminal BRCT domain of Rev1) and knockout MEFs (30,31) were transfected with the HisD reporter construct and Bsd-resistant clones were selected using culture medium with blasticidine (5  $\mu\text{g}/\text{ml}$ ). After 12–14 days, clones were isolated and expanded. Two independent *Rev1* WT and two independent *Rev1*-deficient MEF cell lines containing the reporter construct stably integrated into the genome were cultured for 6 days in culture medium. Then,  $10^6$  cells were cultured in medium with 7.5 mM histidinol and 5  $\mu\text{g}/\text{ml}$  blasticidine to select for HisD revertant (His+Bsd+) clones. In parallel, cells were plated at clonal density (200 cells per 10 cm dish (3 $\times$ )) to correct for the clone forming ability of the cells. After 10–11 days, cells were fixed and stained with methylene blue. Similarly, three independent *Rev1* WT and three independent *Rev1 Brc1* MEF cell lines were used to compare their frequencies of spontaneous His+Bsd+ clones. The HisD reversion assay can be used to analyse replication-associated gene conversion as described previously (32).

### HR assay

To examine the effect of REV1 depletion on HR efficiency, stable REV1 knockdown or negative control 293T cells were transfected with the DR-GFP reporter and I-SceI-IRES-DsRedNLS expression vector (33) by using Lipofectamine 2000 as described (34). Two days later, the frequency of HR-mediated repair events was calculated by analyzing GFP-positive cells out of the DsRed-positive cells in flow cytometry analysis (BD FACSAria). The extent of HR repair in REV1-depleted cells is shown relative to the repair observed in shNC knockdown cells. To examine whether the HR defect observed in REV1-depleted cells is attributed to REV1 depletion, REV1-depleted 293T cells were then transfected with a mixture containing DR-GFP reporter, I-SceI-IRES-DsRedNLS expression vector, and WT or UBMs mutated (UBM\*) Flag-REV1 by using Lipofectamine2000. The extent of repair in cells complemented with WT or UBM\* Flag-REV1 is shown relative to the repair observed in cells transfected with Flag vector. Data from three independent experiments were used to generate the histogram.

### Cell cycle analysis

Immortalized MEF cell lines containing a stably integrated HisD reporter construct were cultured overnight. After washing once with PBS, cells were pulse-labeled with 10  $\mu\text{M}$  Bromodeoxyuridine (BrdU, Millipore) for 30 min at 37°C, rinsed with PBS and continuously cultured in medium containing 5  $\mu\text{M}$  thymidine (Sigma–Aldrich). At different time points, cells were trypsinized and fixed in 70% ethanol. Cells were stained for incorporation of BrdU using a mouse monoclonal antibody against BrdU (Becton Dickinson) and a FITC-conjugated rat anti-mouse antibody (BD bioscience Pharmingen) as described previously (35). Cells were analyzed by flow cytometry (Guava easyCyte HT, Millipore).

### DNA fiber assay

DNA fibers were spread as previously described with some modifications (36). Briefly, for CPT and HU treatments, log-phase cells were pulse-labeled with the modified thymidine analogues iododeoxyuridine (IdU) (100  $\mu\text{M}$ ) for 10 min and then chlorodeoxyuridine (CldU) (100  $\mu\text{M}$ ) for 20 min to indicate the direction of ongoing replication before exposure to CPT (5  $\mu\text{M}$ ) or HU (4 mM) for 5 h. Cells were collected, lysed and spread on microscope slides to obtain single molecule DNA fibers. The labeled replication tracts were detected with primary antibodies against IdU (BD Biosciences, anti-BrdU clone B44) and CldU [Abcam, anti-BrdU BU1/75(ICR1)] and secondary antibodies (Invitrogen, Alexa Fluor 488 goat anti-rat and Alexa Fluor 568 goat anti-mouse). Fibers were imaged using a Leica DM5000B microscope. Length of 100–200 DNA fibers were measured using ImageJ software from two to three independent experiments. *P*-values were obtained from the Mann–Whitney test. For the GFP-REV1 rescue assay or GFP-RAD51 supplementing assay, *Rev1*-deficient MEFs transfected with pEGFP-mREV1 or pEGFP-RAD51 were labeled with IdU and CldU and treated with CPT as above, and then sorted with MoFlo XDP High-Speed Cell Sorter (Beckman Coulter). The sorted GFP positive cells were then used in the DNA fiber spread assay.

### Cell survival assay

A cell survival assay following genotoxic treatments was performed as described previously (25). Briefly, cells were seeded into 6 cm dishes (~200 cells/dish) in triplicate and allowed to adhere for 5 h. The cells were then treated with the indicated amount of CPT or HU for 2 h at 37°C in serum-free medium. After treatment, cells were further incubated in complete medium for 7–10 days. Colonies were fixed and counted. The survival of genotoxin-exposed cells was determined by relating the cloning efficiency to that of an untreated control.

## RESULTS

### REV1 is involved in replication-dependent gene conversion

REV1 protein has recently been shown to play an undefined function in HR in human cells (14). To support that result, we generated stable REV1 knockdown 293T cells and transfected the cells with DR-GFP reporter and I-SceI-IRES-DsRedNLS plasmid. The frequency of HR-mediated repair events was calculated by analyzing GFP-positive cells out of the DsRed-positive cells in flow cytometry analysis. In line with the previous report (14), depletion of REV1 decreases the gene conversion in 293T cells (Figure 1A). To determine whether the HR defect is attributed to REV1 depletion, we co-transfected DR-GFP reporter, I-SceI-IRES-DsRedNLS plasmid and WT or UBMs\* REV1 into REV1-depleted 293T cells. We found that supplementing the REV1-depleted cells with WT REV1 resulted in an increase in the extent of HR repair relative to the Flag vector (Figure 1B), whereas supplementing the REV1-depleted cells with UBMs\* REV1 could not raise the extent of HR repair (Figure 1B). These data support that REV1 is involved in HR.

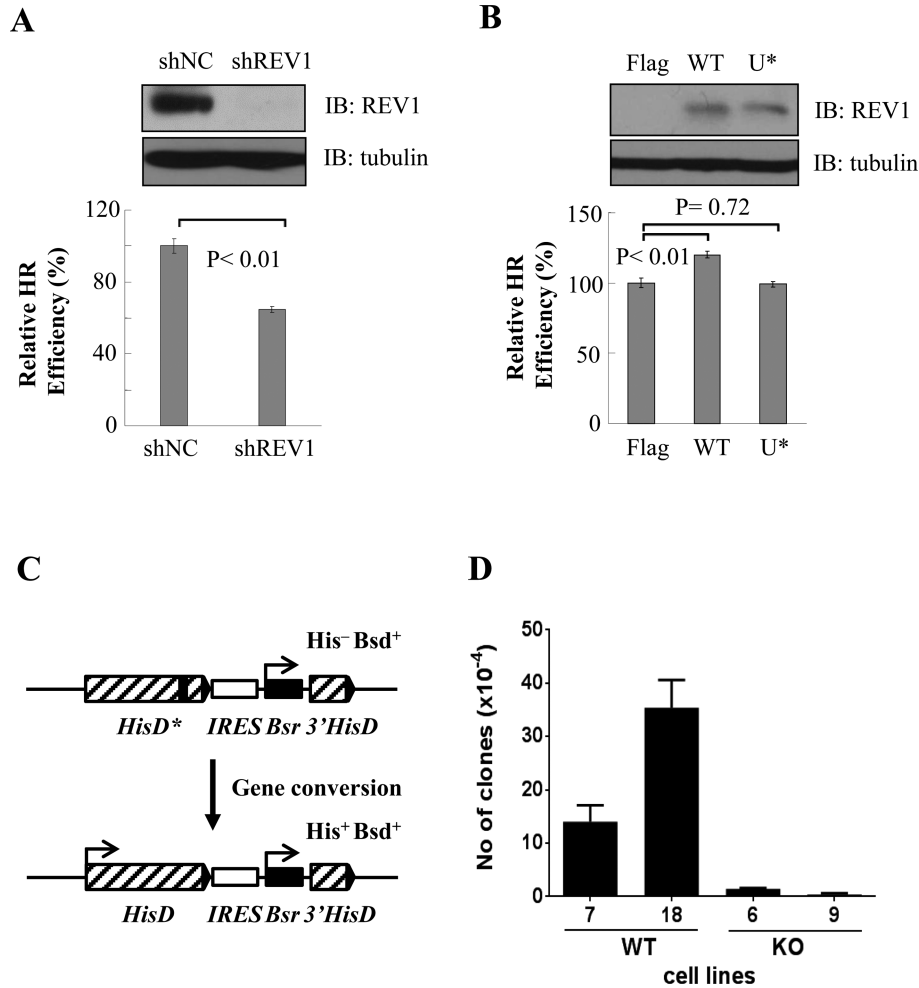


**Figure 1.** REV1 is involved in gene conversion in mammalian cells. (A) REV1-depleted 293T cells were co-transfected with DR-GFP reporter and I-SceI-IRES-DsRedNLS plasmid. Two days later, the frequency of HR-mediated repair events was calculated by analyzing GFP-positive cells out of the DsRed-positive cells in flow cytometry analysis. The extent of repair is shown relative to the repair observed in shRNA-SHC002 (shNC) knockdown cells. Data from three independent experiments were used to generate the histogram. Error bars indicate standard error. *P* values derived from a student's *t*-test are shown at the top. The shREV1-mediated knockdown efficiency was validated by western blot using antibodies against REV1.  $\beta$ -Tubulin: loading control. (B) REV1-depleted 293T cells were co-transfected with DR-GFP reporter, I-SceI-IRES-DsRedNLS plasmid and either Flag or Flag-REV1 (WT) or Flag-REV1 UBMs\* (U\*). The frequency of HR-mediated repair event was calculated as in (A). The extent of repair is shown relative to the repair observed in cells transfected with control Flag vector. The expression of WT or U\* REV1 was validated by western blot using antibodies against REV1. (C) Reporter construct to determine reversion of a defective *HisD* gene (*HisD*<sup>\*</sup>) to a functional *HisD* gene using *HisD* donor sequences (3' *HisD*) in cells. Cells carrying a stably integrated reporter construct are sensitive to histidinol (*His*<sup>-</sup>) and resistant to blasticidin (*Bsd*<sup>+</sup>). *Bsr*, blasticidin selection gene. (D) Frequencies of spontaneous *His*<sup>+</sup>*Bsd*<sup>+</sup> clones in two independent *Rev1* WT (7 and 18) and KO MEFs (6 and 9). Frequencies are corrected for the clone forming ability of the cells. All experiments were carried out in triplicate. Error bars indicate the standard error.

To investigate a role of REV1 in gene conversion during replication, we generated *Rev1* WT and KO MEFs carrying an integrated copy of a *HisD* reporter construct that confers resistance to histidinol (*His*<sup>+</sup>) when the coding sequence of a mutated *Histidinol dehydrogenase* gene (*HisD*<sup>\*</sup>) is restored to WT following recombination with a 3' *HisD* donor (Figure 1C). Since the *HisD*<sup>\*</sup> gene is separated from the 3' *HisD* donor by the *Bsr* gene, cellular resistance to blasticidin and histidinol (*His*<sup>+</sup>*Bsd*<sup>+</sup>) most likely reflects replication-associated gene conversion in these cells. We assayed two independent cell lines for each genotype with the reporter integrated at different genomic loci (Supplementary Figure S1A) and determined that WT cells display much higher frequencies of *His*<sup>+</sup>*Bsd*<sup>+</sup> revertants (varying

from 0.13% to 0.36%) compared with *Rev1*-deficient cells (Figure 1D). The low frequency of *His*<sup>+</sup>*Bsd*<sup>+</sup> revertants in *Rev1*-deficient cells was not caused by a cell cycle defect in *Rev1*-deficient cells, since the *Rev1* WT and KO MEF cell lines displayed a similar cell cycle progression (Supplementary Figure S1B). To further support that the phenotype of apparently reduced gene conversion is related to REV1 deficiency, we examined the frequency of spontaneous *His*<sup>+</sup>*Bsd*<sup>+</sup> clones in MEFs containing a defined deletion in the N-terminal BRCT domain of *Rev1* (*Rev1 Brc1*) (30), which is a completely distinct REV1 mutant. We found that *Rev1 Brc1* cells displayed a similar phenotype as *Rev1* KO cells (Supplementary Figure S1C). Together these re-

sults suggest that gene conversion in mammalian cells might strongly rely on the BRCT region of REV1.

### **RAD18 and the UBMs of REV1 are required for the optimal accumulation of REV1 at damage sites**

HR can occur at DSBs and stalled or collapsed replication forks (37). We then wondered what engages REV1 to these sites to facilitate HR repair. Although yeast Rev1 has been reported to accumulate near DSBs, it remains unclear whether and how mammalian REV1 can target to DSBs. We transfected GFP-REV1 into HCT116 cells and first examined whether REV1 can be recruited to the sites of damage in cells microirradiated with UVA laser, which inflicts, amongst other lesions, DSBs (24,26,38). Within minutes of laser irradiation cells expressing WT GFP-REV1 exhibited the selective accumulation of REV1 at laser tracts (Figure 2A, top panel), colocalizing with  $\gamma$ H2AX, a distinctive marker of DSBs. Since ubiquitination cascades play a key role in the assembly of repair and signaling proteins at sites of DNA damage we asked whether REV1 accumulation at laser damage stripes requires the E3 ubiquitin ligase RAD18 that localizes to DSBs after IR or CPT treatments (16,17). A RAD18 stable knockdown cell line (25) was transfected with GFP-REV1 and microirradiated. The proportion of REV1 accumulation at laser-activated sites was reduced in RAD18-depleted cells (26.4%) compared to control cells (63.1%) and was restored by reintroduction of RAD18 into these cells (60.1%) (Figure 2B and C). Additionally, the average intensity of accumulated GFP-REV1 fluorescence at damage sites was remarkably decreased in RAD18-depleted cells when compared to control cells (Figure 2D). These data suggest that RAD18 plays an important role in recruiting REV1 to DSBs in mammalian cells, in sharp contrast to its reported role in yeast (11).

Since the UBMs in REV1 are required for its binding with ubiquitinated proteins (5), we examined whether the UBMs are required for REV1 accumulation at laser-activated sites in HCT116 cells. Following microirradiation, the percentage of cells with discernible GFP-REV1 accumulation decreased significantly when the cells expressed UBMs mutated (UBM\*) GFP-REV1 (24.7% for UBM\* expressing cells, compared to 53.9% for WT expressing cells) (Figure 2A and E). Additionally, the average intensity of accumulated REV1 fluorescence signal at irradiated sites manifested a significant reduction in cells expressing UBM\* compared to WT REV1 (Figure 2F), indicating that UBMs in REV1 are required for its optimal accumulation at laser-induced sites of damage. In support of this observation enrichment of REV1 after laser microirradiation was also remarkably impaired in U2OS cells when UBMs were mutated (Supplementary Figure S2A). Previous studies have indicated that transiently expressed DsRed-PCNA can be utilized to differentiate S and non-S phase cells as PCNA forms distinct foci in S phase, whereas it shows diffuse expression in non-S phase cells (39,40). To determine whether UBMs are required for optimal REV1 recruitment to microirradiated sites in a cell cycle-dependent manner, we co-transfected WT or UBM\* GFP-REV1 with DsRed-PCNA into U2OS cells. We found that mutation of UBMs led to a reduction of REV1 signals at microirradiated sites in both

S- and non-S phase cells (Supplementary Figure S2B and C). To confirm that REV1 UBMs are required for targeting REV1 to DSBs, we assayed the binding of WT and UBM\* REV1 at I-SceI-induced break sites using a chromatin immunoprecipitation (CHIP) assay. The UBMs in REV1 are indeed necessary for the optimal targeting of REV1 to I-SceI-induced DSBs (Figure 2G). Notably, UBM\* REV1 is still recruited to DSBs to some extent, hinting at the possibility that REV1 assembly at DSBs is also regulated in a UBMs-independent fashion.

### **FANCD2 is required for the optimal accumulation of REV1 at laser-damaged sites**

RAD18 not only stimulates the recruitment of REV1 to laser damage stripes, it is also necessary for CPT-induced recruitment of FANCD2 to chromatin, possibly via RAD18-mediated monoubiquitination of FANCD2 at lysine 561 (FANCD2-mUb) (17,41). FANCD2 is a key factor for resolving replication-associated DSBs and its monoubiquitination at K561 is indispensable for its function (42–44). To examine whether FANCD2-mUb interacts with REV1, we transfected HA-REV1 into 293T cells and harvested the DTBP-crosslinked cell lysates for immunoprecipitation (IP) with an anti-FANCD2 antibody. We found that HA-REV1 was co-immunoprecipitated with FANCD2 in the lysates (Figure 3A). Interestingly, this interaction was enhanced after CPT treatment (Figure 3A), which is expected to increase the FANCD2-mUb level in cells (17). To provide additional support we co-expressed HA-REV1 with a K561R mutated FANCD2 (K561R) or a FANCD2-Ub chimera (a mimic of FANCD2-mUb) in 293T cells and examined their interaction by co-IP. REV1 displayed a stronger interaction with FANCD2-Ub than with the FANCD2 K561R mutant (Figure 3B). In line with this result, REV1 was found to colocalize with FANCD2 in CPT-treated U2OS cells, and CPT treatment led to an increase in REV1 focus formation (Supplementary Figure S3A), while depletion of FANCD2 reduced the REV1 focus formation after CPT treatment. Given that FANCD2 can be recruited to laser-induced DSBs (45) we checked whether depletion of FANCD2 affects REV1 recruitment to laser-activated sites. U2OS cells, depleted for FANCD2 by a *FANCD2* siRNA, were transfected with GFP-REV1 and subjected to microirradiation. As shown in Figure 3C, depletion of FANCD2 significantly reduced REV1 accumulation. Moreover, this accumulation was also impaired in cells treated with three other *FANCD2* siRNAs (Supplementary Figure S3B), suggesting that the decrease of REV1 accumulation triggered by FANCD2 depletion is not the result of siRNA off-target effects. Similar results were obtained in FANCD2 stable knockdown U2OS cells (Supplementary Figure S3C). Additionally, the average intensity of accumulated GFP-REV1 fluorescence at damage sites was decreased in FANCD2-depleted cells when compared to control cells (Supplementary Figure S3D). To provide even more evidence for this, we transfected GFP-REV1 with FANCD2 WT, K561R or FANCD2-Ub into patient-derived FANCD2-defective PD20 cells and examined the recruitment of REV1 to microirradiated sites. We found that expression of FANCD2-Ub or FANCD2 WT signif-

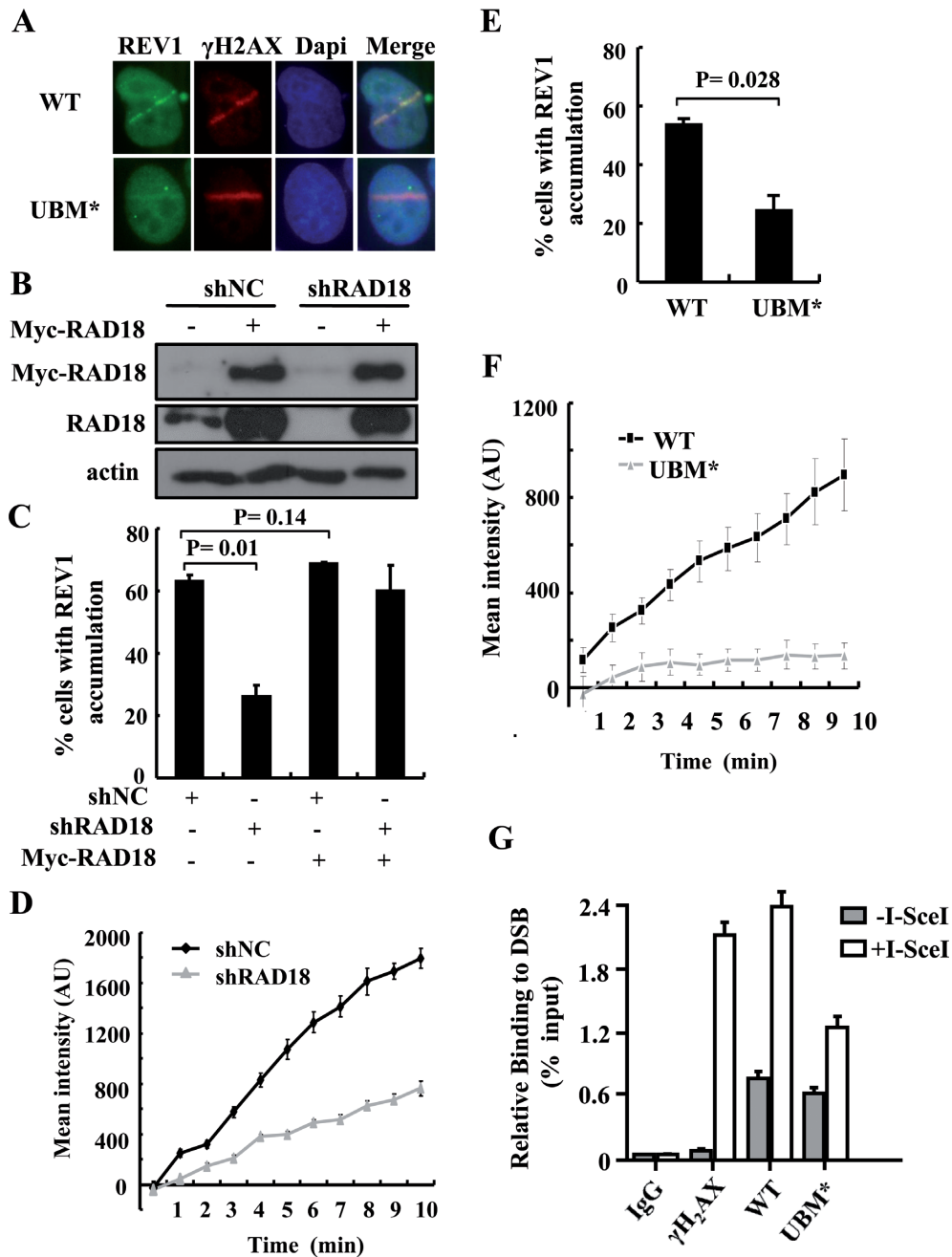


**Figure 2.** RAD18 and UBMs in REV1 are required for the optimal accumulation of GFP-REV1 at HR processing sites. (A) HCT116 cells transfected with WT and UBM\* GFP-REV1 were microirradiated with a pulsed nitrogen laser. Thirty minutes later, cells were fixed and stained with anti- $\gamma$ H2AX antibody. Nuclei were stained with DAPI. (B) and (C) RAD18 stable knockdown and control cells were transfected with GFP-REV1 and Myc-RAD18. (B) The levels of RAD18 and Myc-RAD18 were analyzed by western blot.  $\beta$ -actin, loading control. (C) The cells were microirradiated and the proportion of cells with REV1 accumulation was quantified. Error bars indicate standard error. *P* values derived from a student's *t*-test are shown at the top. (D) Kinetic analysis of GFP-REV1 intensity at laser-irradiated sites in RAD18 knockdown and control cells. Error bars represent standard error based on 10 independent measurements. (E) Percentage of HCT116 cells expressing WT and UBM\* GFP-REV1 in which the protein was localized at microirradiated sites. *P* value derived from a student's *t*-test is shown at the top. (F) Kinetic analysis of WT and UBM\* GFP-REV1 intensity at laser-irradiated sites. (G) UBMs are required for the optimal recruitment of REV1 to I-SceI-induced DSBs in CHIP assay. The y-axis represents the relative enrichment of the indicated proteins compared to the IgG control (after normalization to total input). Mutation of UBMs in REV1 significantly decreases REV1 recruitment to I-SceI-induced DSBs as calculated using a Student's *t*-test (*P* < 0.01). All the data are from three independent experiments ( $\pm$ SEM, *n* = 3).

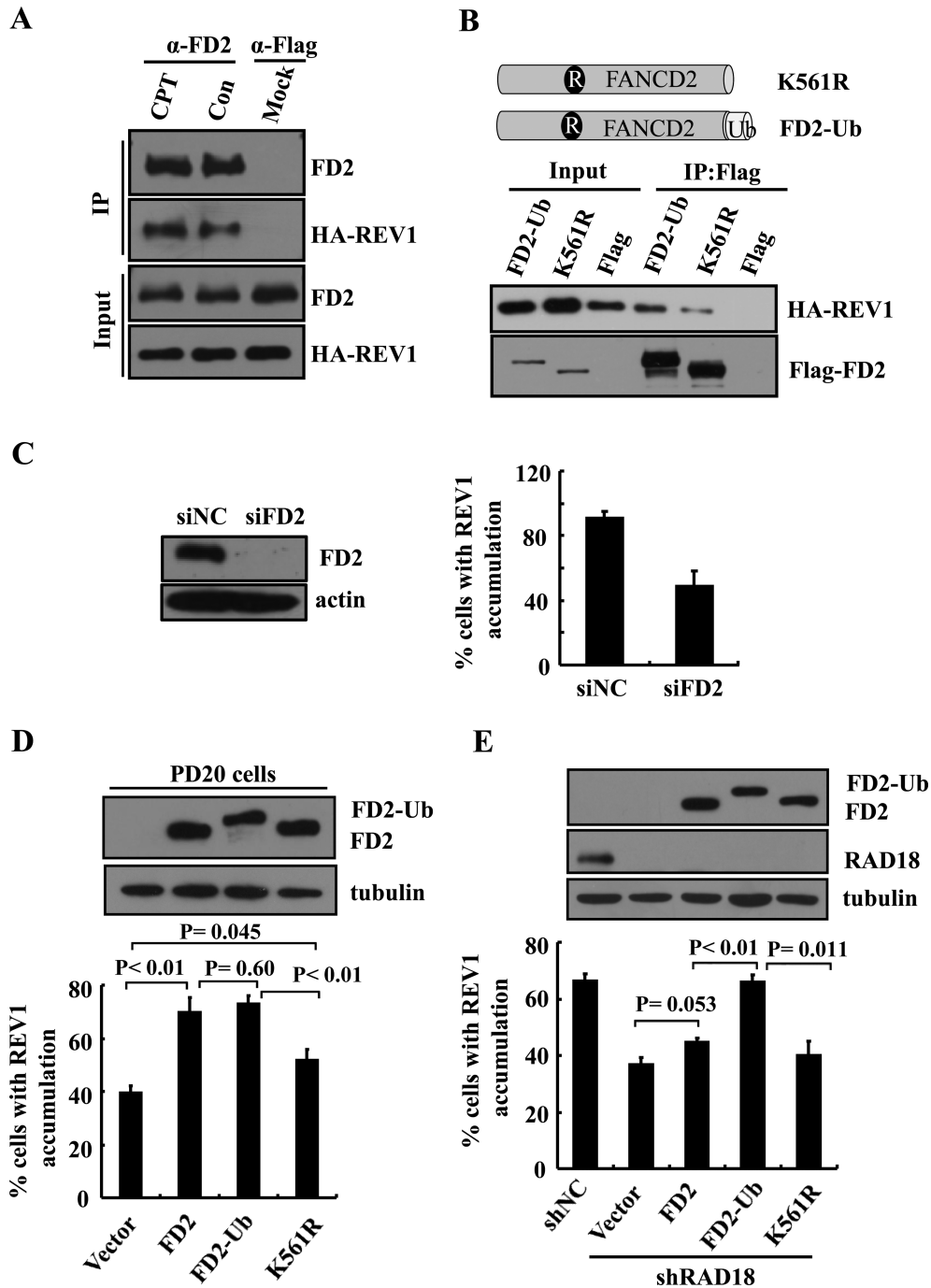


**Figure 3.** FANCD2 physically interacts with REV1 and modulates REV1 recruitment to laser-induced sites of damage. (A) Co-IP showing FANCD2 interacts with REV1. 293T cells transfected with a HA-REV1 expression vector were treated with CPT (5  $\mu$ M) for 2 h and crosslinked with DTBP. The lysates were immunoprecipitated with an anti-FANCD2 antibody. Immunoprecipitates (IP) and inputs were analyzed via western blot using antibodies against HA or FANCD2 (FD2), respectively. Con, untreated cell; Mock, the lysate was immunoprecipitated with an anti-Flag antibody. (B) Top: Schematic diagrams of the FANCD2-K561R mutant (K561R) and FANCD2-Ub (FD2-Ub) constructs. Bottom: Co-IP experiment showing enhanced interaction between FANCD2-Ub and REV1. 293T cells were transfected with plasmids expressing HA-REV1 and SFB-FANCD2-K561R or SFB-FANCD2-Ub and analyzed by co-IP in the presence of EtBr. Immunoprecipitates were analyzed by western blot with antibodies against HA or Flag. (C) FANCD2 depletion impairs the recruitment of REV1 to laser-activated sites. U2OS cells were transfected with *siFANCD2* (siFD2) or siNC. Three days later, the cells were harvested and the levels of FANCD2 were detected by western blot.  $\beta$ -Actin, loading control. The cells were further transfected with GFP-REV1 and microirradiated. The proportion of cells with REV1 accumulation was quantified. (D) PD20 cells were transfected with GFP-REV1 and FANCD2 WT (FD2), K561R or a FD2-Ub chimera. Levels of FANCD2 in cell lysates were detected by western blot with antibodies against Flag.  $\beta$ -tubulin, loading control. Cells were microirradiated. The proportion of cells containing accumulated REV1 was quantified. (E) Complementation with a FANCD2-Ub chimera can rescue the aberrant REV1 recruitment in the RAD18-depleted cells. RAD18 stable knockdown or control cells were transfected with GFP-REV1 and FD2 WT, K561R or a FD2-Ub chimera. Levels of FANCD2 and RAD18 in cell lysates were detected by western blot with antibodies against either Flag or RAD18.  $\beta$ -Tubulin, loading control. Cells were microirradiated. The proportion of cells with REV1 accumulation was quantified. Error bars indicate standard error. *P* values derived from a student's *t*-test are shown at the top.

icantly increased REV1 enrichment, while expression of FANCD2-K561R exhibited less effect (Figure 3D). These data are consistent with the above finding that REV1 had a stronger interaction with FANCD2-Ub than FANCD2-K561R, suggesting that FANCD2-mUb plays an important role in recruiting REV1 to laser-induced lesions. Importantly, the *siFANCD2*-depleted cells manifested no obvious reduction in REV1 focus formation when exposed to UV irradiation ( $P = 0.46$ ) (Supplementary Figure S3E), suggesting that FANCD2 stimulates REV1 focus formation in a DNA lesion-specific fashion, i.e. specifically to DSBs. Additionally, we found that mutation of the REV1 UBM domains affected its association with FANCD2-Ub but not unmodified FANCD2 (Supplementary Figure S4). Moreover, depletion of REV1 did not impair FANCD2 recruitment to laser microirradiated sites (Supplementary Figure S5A and B), in agreement with the notion that REV1 functions downstream of FANCD2 after microirradiation. Notably, depletion of FANCD2 in U2OS cells reduced REV1 accumulation at microirradiated sites in both S- and non-S phase cells (Supplementary Figure S5C). Further, co-IP experiments showed that REV1 also interacts with FANCI, a FANCD2 partner which can be monoubiquitinated after different DNA damage treatments (46) (Supplementary Figure S6), indicating that FANCI might regulate REV1 function(s), too.

To directly test whether the impaired recruitment of REV1 to laser-induced sites in RAD18-depleted cells (Figure 2C) was due to a lack of FANCD2-mUb we expressed a FANCD2-Ub chimera, FANCD2 WT or K561R in RAD18-depleted cells (Figure 3E) and assayed for REV1 recruitment to laser tracts. We found that complementation with a FANCD2-Ub chimera, but not a FANCD2 WT or K561R, completely rescued the aberrant REV1 recruitment in RAD18-depleted cells (65.9% for FANCD2-Ub expressing cells, compared to 44.6% or 39.8% for FANCD2 WT or K561R-expressing cells) (Figure 3E). In addition, the reduction of REV1 signal intensity at damage sites in the RAD18-depleted cells was alleviated after supplementing with FANCD2-Ub chimera (Supplementary Figure S7). These data indicate that FANCD2-mUb functions downstream of RAD18 to regulate REV1 recruitment to laser-activated sites.

#### **Rev1-deficient cells are hypersensitive to CPT treatment**

RAD18 and FANCD2 have been implicated in cellular responses to CPT, a drug that causes replication-associated DSBs (17). Given that FANCD2 regulates REV1 recruitment to laser-induced sites we investigated the role of REV1 in the cellular response to CPT exposure. We exposed *Rev1* WT and KO MEFs to CPT and found that *Rev1* KO MEFs exhibited enhanced sensitivity to CPT treatment (Figure 4A), indicating a role of REV1 in the response to replication-associated DSBs. Similar results were obtained in REV1-depleted U2OS cells (Supplementary Figure S8) and in *Rev1* WT and KO MEFs exposed to HU (Figure 4B). To determine whether REV1 and FANCD2 promote cellular resistance to CPT treatment through a common pathway we examined the effect of FANCD2 depletion on cellular survival following DNA damage in *Rev1* KO MEFs. Al-

though depletion of FANCD2 significantly sensitized WT cells to CPT exposure ( $P < 0.05$ ) its depletion did not enhance the CPT sensitivity of *Rev1* KO cells (Figure 4C and D). This data indicates that FANCD2 and REV1 likely contribute to cellular CPT tolerance, at least in part, through a common pathway.

#### **BRCA1 and BRCA2 modulate REV1 accumulation at laser-damaged sites**

FANCD2 has been reported to interact with BRCA1 and BRCA2 generating a FANCD2/BRCA supercomplex that stabilizes the RAD51 filament formation at stalled replication forks after CPT treatment (36,47). Recently, REV1 was also shown to associate with BRCA1 (10). To examine whether BRCA1 modulates REV1 assembly at DSB sites, BRCA1-depleted U2OS cells were transfected with GFP-REV1 and accumulation of REV1 at laser-induced tracks was analyzed. Depletion of BRCA1 led to an obvious reduction of REV1 accumulation at laser-damaged sites compared to control cells (40.0% for *siBRCA1* treated cells, compared to 58.0% for control cells) (Figure 5A). Similarly, depletion of BRCA2 also significantly reduced REV1 recruitment (32.8% in *siBRCA2*-treated cells, compared to 60.8% for control cells) (Figure 5B). These results suggest that the FANCD2/BRCA supercomplex is important for the recruitment of REV1 to sites where HR is processed. Given that signaling pathways are often not linear in the cellular response to DNA damage, we also examined whether knocking down REV1 would affect BRCA1 recruitment to laser-induced sites of damage. We found that depletion of REV1 does not impair BRCA1 recruitment after microirradiation (Figure 5C and D).

#### **REV1 protects nascent DNA strands at disturbed replication forks**

Since FANCD2-mUb and BRCA1 can act in replication fork stabilization independent of DSB repair (36,48) we asked whether REV1 plays a similar role in the protection of nascent DNA tracts at stalled replication forks after CPT treatment, using a DNA fiber spreading resection assay (49). Cells were pulse-labeled with IdU for 10 min followed by CldU for 20 min prior to CPT treatment for 5 h, and then by DNA fiber spreading (Figure 6A). The length of newly synthesized DNA strands (red fluorescent IdU and green fluorescent CldU) before exposure to CPT was monitored. In *Rev1* WT MEFs the median fiber length remained intact with or without CPT treatment (12.15 and 12.33  $\mu\text{m}$ , respectively,  $P = 0.2648$ ) (Figure 6B, upper panel). Conversely, in *Rev1* KO MEFs nascent tracks substantially shortened after CPT exposure compared to the unperturbed controls (8.65 and 11.79  $\mu\text{m}$  respectively,  $P < 0.0001$ ) (Figure 6B, bottom panel). Similar results were obtained following exposure of the cells to HU (Supplementary Figure S9). To directly assess whether fork protection requires REV1 we transfected *Rev1* KO MEFs with either GFP-REV1 or GFP and analyzed nascent replication tracts in the sorted GFP-positive cells after CPT treatment. Replication stalling failed to promote dramatic shortening of the nascent tracks in *Rev1* KO MEFs complemented with GFP-REV1 (14.49  $\mu\text{m}$ ) compared to cells complemented with

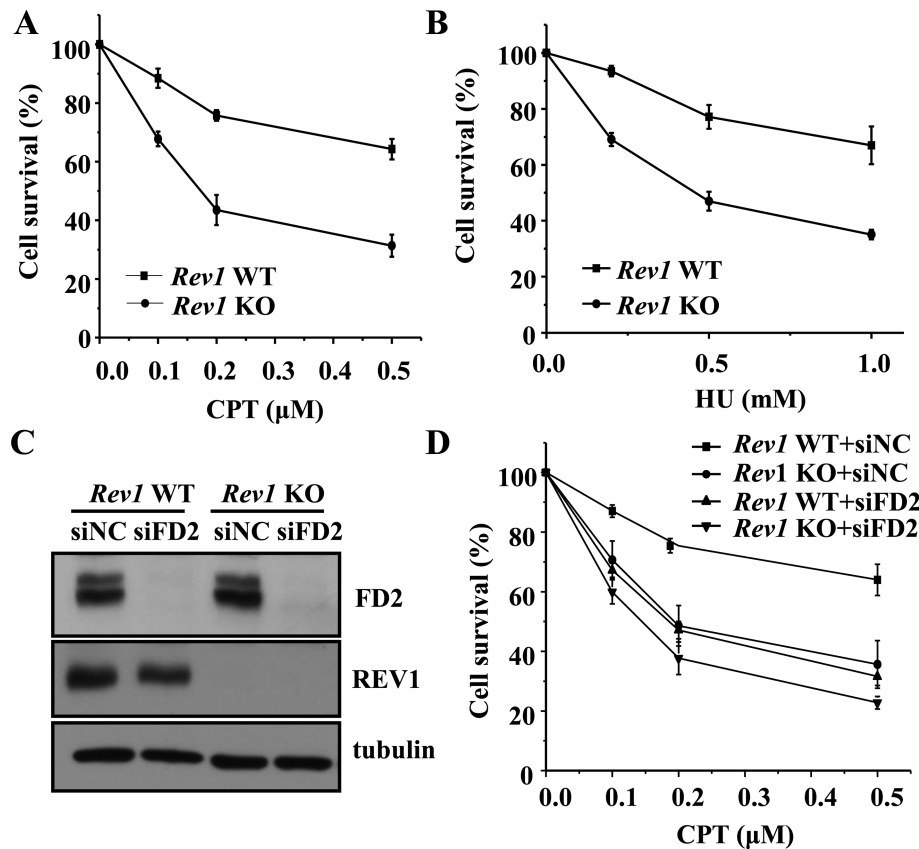


**Figure 4.** REV1 is involved in cellular response to CPT exposure. (A) WT and *Rev1* KO MEFs were treated with CPT for 2 h and further incubated in fresh medium for 7–10 days. The number of cell clones was determined. Surviving fraction was expressed as a percentage of mock-treated cells. Error bars: SD,  $n = 3$ . (B) WT and *Rev1* KO MEFs were treated with HU for 2 h. Cell survival was analyzed as in (A). (C) WT and *Rev1* KO MEFs were transfected with *siFancd2* (siFD2) or siNC. The levels of REV1 and FANCD2 were analyzed by western blot.  $\beta$ -Tubulin, loading control. (D) WT and *Rev1* KO MEFs transfected with *siFancd2* (siFD2) or siNC, were treated with CPT for 2 h and analyzed as in (A). Values are means of three independent experiments. Error bars indicate standard error. Depletion of FANCD2 in *Rev1* KO MEFs did not enhance cellular sensitivity to CPT as calculated using a Student's *t*-test ( $P > 0.05$ ).

only GFP (11.07  $\mu\text{m}$ ) ( $P < 0.0001$ ; Figure 7A, upper and middle panels; Figure 7B).

Given that the fork instability in FANCD2-deficient cells is attributable to perturbed RAD51 filament stabilization (36) we asked whether a similar mechanism is responsible for the nascent tracts protection defect in *Rev1* KO MEFs. To test this possibility we first checked whether REV1 associates with RAD51 as is the case with other components of the FANCD2/BRCA supercomplex. Flag-REV1 and GFP-RAD51 expression vectors were co-transfected into 293T cells and Flag-REV1 was immunoprecipitated. RAD51 was found to be co-precipitated even in the presence of the DNA intercalator EtBr, indicating that their interaction is not mediated by DNA (Supplementary Figure S10A). Since overexpression of RAD51 promotes stable RAD51 filament assembly upon fork stalling following CPT exposure (50), we also transfected either GFP or GFP-RAD51 into *Rev1* KO cells as above (Supplementary Figure S10B) and compared the lengths of their nascent tracts after CPT treatment (Figure 7A, upper and bottom panels). We observed that overexpression of GFP-RAD51 but not GFP rendered nascent tracts in *Rev1*-deficient cells resistant to degradation, maintaining replication tract lengths comparable to

those observed in the cells in the absence of CPT treatment (Figure 7A, bottom panel; 14.42 and 14.32  $\mu\text{m}$  respectively,  $P = 0.8519$ ). Hence, fork instability caused by REV1 deficiency can be compensated by RAD51 overexpression, analogous to that observed in FANCD2-defective cells (36). Furthermore, previous studies have indicated that MRE11 is responsible for nascent DNA strands shortening in the absence of FANCD2, BRCA2 and RAD51 at stalled forks (36,48,49). To check whether MRE11 is also the nuclease that degrades nascent DNA strands in the absence of REV1, we depleted Mre11 in *Rev1*-deficient cells using *siMre11* and measured the nascent DNA track lengths. We found that depletion of Mre11 blocked nascent track shortening upon CPT treatment (Supplementary Figure S11; 14.20 and 14.29  $\mu\text{m}$  respectively,  $P = 0.8493$ ), indicating that MRE11 promotes fork degradation in the absence of REV1. Taken together, the data suggest that downstream of FANCD2-mUb REV1 accumulates at replication forks to positively regulate replication tract stability.

## DISCUSSION

Persistently arrested DNA replication can threaten the viability of dividing cells. TLS utilizes specialized DNA poly-

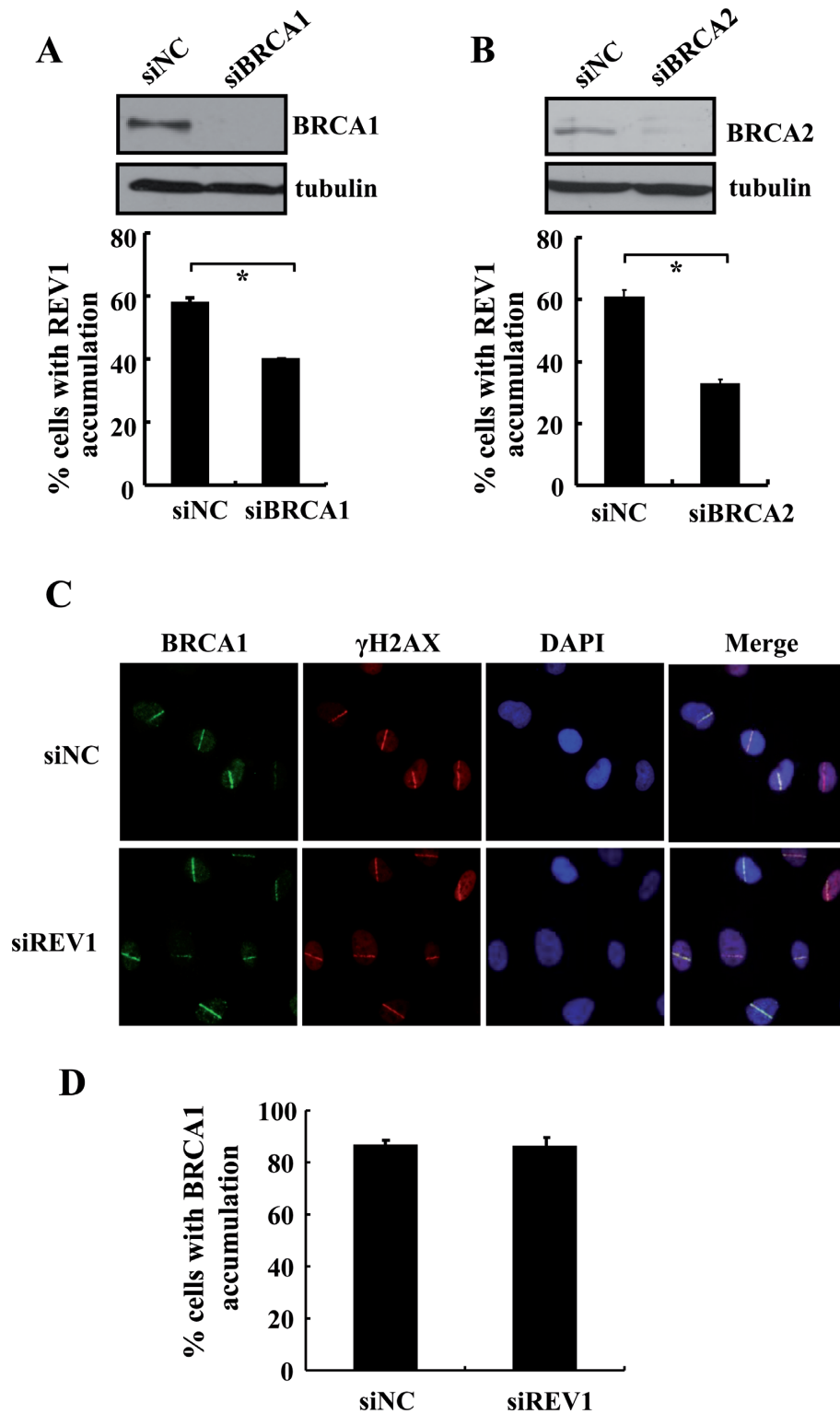


**Figure 5.** BRCA1 and BRCA2 modulate the assembly of REV1 at laser-induced sites of damage. (A) U2OS cells were transfected with *siBRCA1* or siNC. Three days later, the level of BRCA1 was analyzed by western blot. Microirradiation was performed as in Figure 3C. A Student's *t*-test was used to calculate the *P* value ( $P < 0.05$ ). (B) U2OS cells were transfected with *siBRCA2* or siNC. The level of BRCA2 was analyzed by western blot. Microirradiation was performed as in Figure 3C.  $\beta$ -Tubulin, loading control. (C) U2OS cells were transfected with *siREV1* or siNC. Three days later, the cells were microirradiated. Thirty minutes later, cells were fixed and stained with antibodies against BRCA1 and  $\gamma$ H2AX. Nuclei were stained with DAPI. (D) The proportion of cells with BRCA1 accumulation was quantified. Error bars indicate standard error.

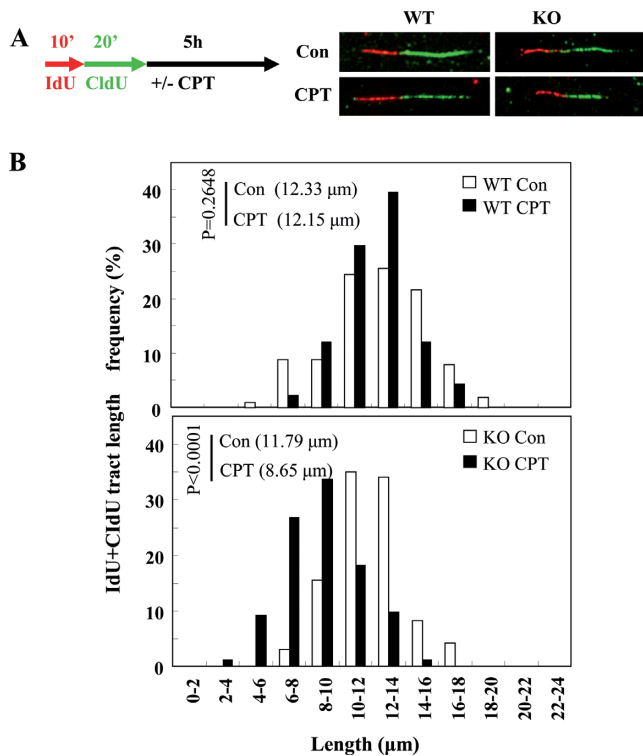


**Figure 6.** REV1 protects nascent replication tracts at stalled replication forks after exposure to CPT. (A) Scheme of experimental design for fork stability assay in *Rev1* WT and KO MEFs. Length of nascent replication tracts (labeled with IdU and CldU) was measured by DNA spreading after 5 h of replication stalling with CPT. Representative, individual DNA fibers for each experimental condition are shown. (B) Nascent tract length distributions were measured in WT (Top panel) and KO (Bottom panel) with 5  $\mu$ M CPT or not. Median lengths of nascent replication tracts are given in parentheses. *P*-value is derived from the Mann-Whitney test. The nascent tract lengths were comparable in mock-treated WT and KO cells.

merases to catalyze DNA synthesis past sites of base damage and unusual structures such as G quadruplexes (3) to alleviate the threat, but at the expense of increased mutagenesis. Compelling evidence from a variety of systems suggests that TLS polymerases can also be utilized during HR (13,51), while REV1 may coordinate the recruitment of TLS polymerases during HR-associated repair synthesis (13). However, little is known about how REV1 is targeted to the sites where HR are processed. In addition, it remains elusive whether REV1 plays other roles at stalled replication forks.

Using a reporter system to analyze DNA template switching we determined that REV1, via its Brct domain, plays an important role in replication-associated gene conversion, which might be related to its interaction with RAD51 and/or Rad5, two central components of the template switching pathway (52,53). We then searched for factors that engage REV1 to HR processing sites. Our results show that optimal assembly of mouse REV1 at laser-induced DSBs partially depends on RAD18 and the functional UBMs of REV1. Mutation of UBMs in REV1 or depletion of RAD18 significantly reduced the recruitment of REV1 to laser damage stripes in terms of signal intensity and percentage of positive nuclei. Interestingly, depletion

of FANCD2, which colocalizes with REV1 in nuclear foci following replication fork arrest (15) also decreased REV1 accumulation. In view of the fact that RAD18 can be recruited to DSBs and is essential for appropriate FANCD2-mUb formation after CPT treatment (17) we complemented a RAD18 knockdown stable cell line with a mimic of FANCD2-mUb which manifests an enhanced interaction with REV1, and determined that REV1 recruitment was significantly recovered. These results indicate that RAD18 facilitates REV1 recruitment to laser-induced DSBs, at least in part, through promoting FANCD2-mUb. Therefore, although FANCD2-mUb is not required for REV1 accumulation at UV-stalled replication forks and associated mutagenesis (8), it is critical for optimal recruitment of REV1 protein to DSBs. This mode of regulation is mechanistically distinct from the previously reported connections between REV1 and the FA pathway, in which the recruitment of REV1 to damage sites following UV or cisplatin treatment requires an intact FA core complex but is independent of FANCD2-mUb (9). Hence, REV1 is likely to be differently regulated in specific contexts to protect the genome against different types of DNA lesions. In support of this observation REV1 and FANCD2 are found to promote cellular resistance to CPT treatment through a common pathway. Notably, REV1 recruitment to laser-induced DSBs can still be detected in some of REV1 UBMs\*-expressing cells, suggesting that an additional UBMs-independent mechanism(s) likely contributes to this process, which might coordinate with the UBMs-dependent fashion to ensure optimal REV1 enrichment.

BRCA1 has recently been shown to interact with RAD18 and REV1 (10). Notably, we found that depletion of BRCA1 and BRCA2 also impairs REV1 recruitment to laser tracts. Given that BRCA1 and BRCA2 can rapidly relocalize to stalled replication forks (36) and BRCA1 is required for RAD18 chromatin binding (10), it is conceivable that BRCA1 functions either upstream of RAD18 or through association with REV1 (10) to regulate REV1 assembly. Combined with the fact that FANCD2 associates in complexes with BRCA1 as well as BRCA2 (54) it is plausible that recruitment of REV1 to DSBs is generally regulated by the FANCD2/BRCA complex, which might therefore modulate the function of REV1 in eukaryotes near DSBs.

Although FANCD2 can be activated at DSBs (42) it is not a canonical HR factor (55). The FA/BRCA network was recently reported to play an unexpected repair-independent function in preventing degradation of nascent DNA strands at stalled replication forks (36). Our present observation that REV1 recruitment to laser-induced sites of damage is regulated by the FANCD2/BRCA complex also hints at the possibility that REV1 may be required to maintain the integrity of nascent replication tracts. To investigate the involvement of REV1 in this process we monitored the stability of nascent replication tracts in *Rev1*-deficient MEFs. Replication stalling elicited by CPT and HU causes a dramatic shortening of the median nascent tract length in *Rev1* KO cells compared either to mock treatment or to WT controls, which could be rescued by supplementing with GFP-REV1 or GFP-RAD51 or *siMRE11*. These results are analogous to recent findings in FANCD2-defective cells (36) indicating that REV1 apparently stabilizes RAD51 to

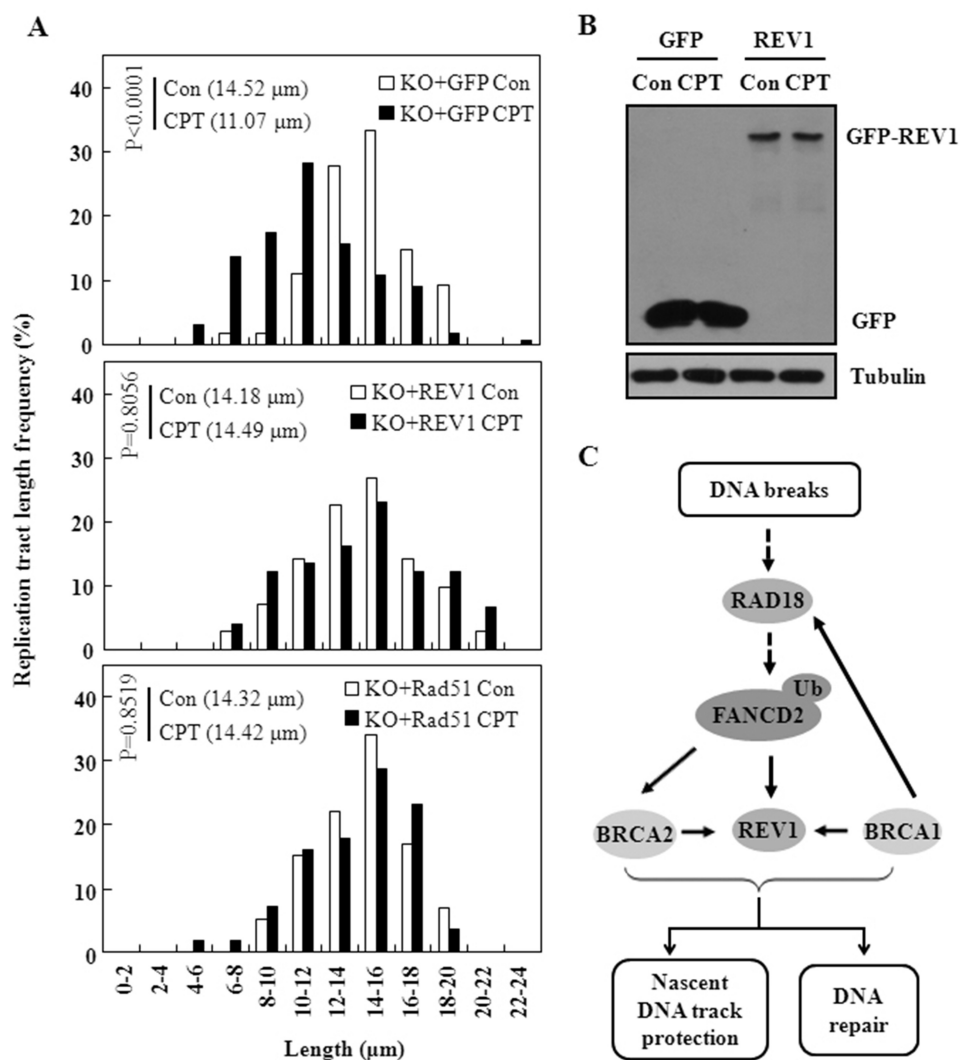


**Figure 7.** REV1 protects nascent replication tracts intact by stabilizing RAD51 filaments. (A) Complementation of REV1 or RAD51 in *Rev1* KO MEFs can rescue the replication fork instability upon CPT. *Rev1* KO MEFs transfected with GFP-REV1, or GFP-RAD51 or GFP were labeled with IdU and CIdU and then treated with CPT. GFP-positive cells were sorted with MoFlo XDP High-Speed Cell Sorter (Beckman Coulter) for the DNA spreading assay. Nascent tract length distributions in these cells were measured as in Figure 6. (B) Expression of GFP or GFP-REV1 in the sorted *Rev1* KO MEFs was detected through western blot by immunoblotting with anti-GFP antibodies.  $\beta$ -tubulin was used as loading control. (C) Model of REV1 targeting to DNA breaks to prevent chromosome instability.

protect nascent strands from degradation by MRE11 during perturbed DNA replication. Alternatively, given that the role of RAD51 in postreplication repair is well established (48) and TLS polymerases can assist DNA synthesis from strand invasion intermediates of HR (56), association of REV1 with RAD51 may facilitate REV1-regulated access of TLS polymerases to HR intermediates (13), which can extend and thus prevents the nascent DNA from excessive nucleolytic degradation. In the absence of REV1, the invaded strand is unstable and will be degraded except when Rad51 is over-expressed.

Accordingly, we propose the following overall model (Figure 7C): Upon DNA breaks, RAD18 is rapidly relocalized to DSBs to facilitate FANCD2-mUb (17), which then promotes optimal REV1 accumulation. This recruitment is also modulated by BRCA1 and BRCA2. Once recruited,

REV1 either functions in DNA repair, such as HR, or cooperates with FANCD2-mUb, BRCA1 and BRCA2 to block nascent replication tracts from degradation in response to replication stress.

In summary, we have identified a novel role for REV1 in protection of nascent replication tracts against nucleolytic degradation, which it shares with other FANCD2-interacting proteins such as BRCA1 and BRCA2. We also established that gene conversion in mammalian cells is dependent on the Brc1 domain of REV1. Further studies will be required to clarify the detailed function(s) of REV1 in replication-dependent gene conversion and its contribution to genome instability during cancer development.

#### SUPPLEMENTARY DATA

Supplementary Data are available at NAR Online.

## ACKNOWLEDGEMENTS

The authors thank Drs Larry Kartinz, Niall Howlett, Junjie Chen, Yanbin Zhang, Hailong Wang for reagents, Dr David Chen and Shiya Wang for help on microirradiation, Dr Katharina Schlacher for instructions on DNA fiber assay, Dr Xiaoyan Sun and Yan Jia for help with cell culture, the Fanconi Anemia Research Fund for PD20 cells.

## FUNDING

Chinese National 973 Project [2013CB945000, 2011CB944302 to C.G, 2012CB944702, 2011CB965003 to T.-S.T]; National Natural Science Foundation of China [31471331, 31170730 to C.G., 81371415 to T.-S.T, 81101489 to Z.L.]; Strategic Priority Research Program of the CAS [XDB14030302]; CAS/SAFEA International Partnership Program for Creative Research Teams; State Key Laboratory of Membrane Biology. Funding for open access charge: Chinese National 973 Project [2013CB945000].

*Conflict of interest statement.* None declared.

## REFERENCES

- Guo, C., Kosarek-Stancel, J.N., Tang, T.S. and Friedberg, E.C. (2009) Y-family DNA polymerases in mammalian cells. *Cell Mol. Life Sci.*, **66**, 2363–2381.
- Waters, L.S., Minesinger, B.K., Wilttrout, M.E., D'Souza, S., Woodruff, R.V. and Walker, G.C. (2009) Eukaryotic translesion polymerases and their roles and regulation in DNA damage tolerance. *Microbiol. Mol. Biol. Rev.*, **73**, 134–154.
- Sale, J.E., Lehmann, A.R. and Woodgate, R. (2012) Y-family DNA polymerases and their role in tolerance of cellular DNA damage. *Nat. Rev. Mol. Cell Biol.*, **13**, 141–152.
- Tissier, A., Kannouche, P., Reck, M.P., Lehmann, A.R., Fuchs, R.P. and Cordonnier, A. (2004) Co-localization in replication foci and interaction of human Y-family members, DNA polymerase pol eta and REV1 protein. *DNA Repair*, **3**, 1503–1514.
- Guo, C., Tang, T.S., Bienko, M., Parker, J.L., Bielen, A.B., Sonoda, E., Takeda, S., Ulrich, H.D., Dikic, I. and Friedberg, E.C. (2006) Ubiquitin-binding motifs in REV1 protein are required for its role in the tolerance of DNA damage. *Mol. Cell Biol.*, **26**, 8892–8900.
- Guo, C., Fischhaber, P.L., Luk-Paszyc, M.J., Masuda, Y., Zhou, J., Kamiya, K., Kisker, C. and Friedberg, E.C. (2003) Mouse Rev1 protein interacts with multiple DNA polymerases involved in translesion DNA synthesis. *EMBO J.*, **22**, 6621–6630.
- Kim, H., Yang, K., Dejsuphong, D. and D'Andrea, A.D. (2012) Regulation of Rev1 by the Fanconi anemia core complex. *Nat. Struct. Mol. Biol.*, **19**, 164–170.
- Mirchandani, K.D., McCaffrey, R.M. and D'Andrea, A.D. (2008) The Fanconi anemia core complex is required for efficient point mutagenesis and Rev1 foci assembly. *DNA Repair*, **7**, 902–911.
- Ghosal, G. and Chen, J. (2013) DNA damage tolerance: a double-edged sword guarding the genome. *Transl. Cancer Res.*, **2**, 107–129.
- Tian, F., Sharma, S., Zou, J., Lin, S.Y., Wang, B., Rezvani, K., Wang, H., Parvin, J.D., Ludwig, T., Canman, C.E. *et al.* (2013) BRCA1 promotes the ubiquitination of PCNA and recruitment of translesion polymerases in response to replication blockade. *Proc. Natl. Acad. Sci. U.S.A.*, **110**, 13558–13563.
- Hirano, Y. and Sugimoto, K. (2006) ATR homolog Mec1 controls association of DNA polymerase zeta-Rev1 complex with regions near a double-strand break. *Curr. Biol.*, **16**, 586–590.
- Okada, T., Sonoda, E., Yoshimura, M., Kawano, Y., Saya, H., Kohzaki, M. and Takeda, S. (2005) Multiple roles of vertebrate REV genes in DNA repair and recombination. *Mol. Cell Biol.*, **25**, 6103–6111.
- Kane, D.P., Shusterman, M., Rong, Y. and McVey, M. (2012) Competition between replicative and translesion polymerases during homologous recombination repair in *Drosophila*. *PLoS Genet.*, **8**, e1002659.
- Sharma, S., Hicks, J.K., Chute, C.L., Brennan, J.R., Ahn, J.Y., Glover, T.W. and Canman, C.E. (2012) REV1 and polymerase zeta facilitate homologous recombination repair. *Nucleic Acids Res.*, **40**, 682–691.
- Niedzwiedz, W., Mosedale, G., Johnson, M., Ong, C.Y., Pace, P. and Patel, K.J. (2004) The Fanconi anaemia gene FANCC promotes homologous recombination and error-prone DNA repair. *Mol. Cell*, **15**, 607–620.
- Huang, J., Huen, M.S., Kim, H., Leung, C.C., Glover, J.N., Yu, X. and Chen, J. (2009) RAD18 transmits DNA damage signalling to elicit homologous recombination repair. *Nat. Cell Biol.*, **11**, 592–603.
- Palle, K. and Vaziri, C. (2011) Rad18 E3 ubiquitin ligase activity mediates Fanconi anemia pathway activation and cell survival following DNA Topoisomerase 1 inhibition. *Cell Cycle*, **10**, 1625–1638.
- Bienko, M., Green, C.M., Crosetto, N., Rudolf, F., Zapart, G., Coull, B., Kannouche, P., Wider, G., Peter, M., Lehmann, A.R. *et al.* (2005) Ubiquitin-binding domains in Y-family polymerases regulate translesion synthesis. *Science*, **310**, 1821–1824.
- Wei, L., Lan, L., Hong, Z., Yasui, A., Ishioka, C. and Chiba, N. (2008) Rapid recruitment of BRCA1 to DNA double-strand breaks is dependent on its association with Ku80. *Mol. Cell Biol.*, **28**, 7380–7393.
- Jakobs, P.M., Sahaayaruban, P., Saito, H., Reifsteck, C., Olson, S., Joenje, H., Moses, R.E. and Grompe, M. (1996) Immortalization of four new Fanconi anemia fibroblast cell lines by an improved procedure. *Somatic Cell Mol. Genet.*, **22**, 151–157.
- Akagi, J., Masutani, C., Kataoka, Y., Kan, T., Ohashi, E., Mori, T., Ohmori, H. and Hanaoka, F. (2009) Interaction with DNA polymerase eta is required for nuclear accumulation of REV1 and suppression of spontaneous mutations in human cells. *DNA Repair*, **8**, 585–599.
- Hicks, J.K., Chute, C.L., Paulsen, M.T., Ragland, R.L., Howlett, N.G., Gueranger, Q., Glover, T.W. and Canman, C.E. (2010) Differential roles for DNA polymerases eta, zeta, and REV1 in lesion bypass of intrastand versus interstrand DNA cross-links. *Mol. Cell Biol.*, **30**, 1217–1230.
- Bruun, D., Folias, A., Akkari, Y., Cox, Y., Olson, S. and Moses, R. (2003) siRNA depletion of BRCA1, but not BRCA2, causes increased genome instability in Fanconi anemia cells. *DNA Repair*, **2**, 1007–1013.
- Uematsu, N., Weterings, E., Yano, K., Morotomi-Yano, K., Jakob, B., Taucher-Scholz, G., Mari, P.O., van Gent, D.C., Chen, B.P. and Chen, D.J. (2007) Autophosphorylation of DNA-PKCS regulates its dynamics at DNA double-strand breaks. *J. Cell Biol.*, **177**, 219–229.
- Zhang, X., Lv, L., Chen, Q., Yuan, F., Zhang, T., Yang, Y., Zhang, H., Wang, Y., Jia, Y., Qian, L. *et al.* (2013) Mouse DNA polymerase kappa has a functional role in the repair of DNA strand breaks. *DNA Repair*, **12**, 377–388.
- Lan, L., Nakajima, S., Oohata, Y., Takao, M., Okano, S., Masutani, M., Wilson, S.H. and Yasui, A. (2004) In situ analysis of repair processes for oxidative DNA damage in mammalian cells. *Proc. Natl. Acad. Sci. U.S.A.*, **101**, 13738–13743.
- Guo, C., Sonoda, E., Tang, T.S., Parker, J.L., Bielen, A.B., Takeda, S., Ulrich, H.D. and Friedberg, E.C. (2006) REV1 protein interacts with PCNA: significance of the REV1 BRCT domain in vitro and in vivo. *Mol. Cell*, **23**, 265–271.
- Lv, L., Wang, F., Ma, X., Yang, Y., Wang, Z., Liu, H., Li, X., Liu, Z., Zhang, T., Huang, M. *et al.* (2013) Mismatch repair protein MSH2 regulates translesion DNA synthesis following exposure of cells to UV radiation. *Nucleic Acids Res.*, **41**, 10312–10322.
- Pei, H., Zhang, L., Luo, K., Qin, Y., Chesni, M., Fei, F., Bergsagel, P.L., Wang, L., You, Z. and Lou, Z. (2011) MMSET regulates histone H4K20 methylation and 53BP1 accumulation at DNA damage sites. *Nature*, **470**, 124–128.
- Jansen, J.G., Tsaalbi-Shtylik, A., Langerak, P., Calleja, F., Meijers, C.M., Jacobs, H. and de Wind, N. (2005) The BRCT domain of mammalian Rev1 is involved in regulating DNA translesion synthesis. *Nucleic Acids Res.*, **33**, 356–365.
- Jansen, J.G., Tsaalbi-Shtylik, A., Hendriks, G., Gali, H., Hendel, A., Johansson, F., Erixon, K., Livneh, Z., Mullenders, L.H., Haracska, L.

- et al.* (2009) Separate domains of Rev1 mediate two modes of DNA damage bypass in mammalian cells. *Mol. Cell Biol.*, **29**, 3113–3123.
32. Li,Z., Xiao,W., McCormick,J.J. and Maher,V.M. (2002) Identification of a protein essential for a major pathway used by human cells to avoid UV- induced DNA damage. *Proc. Natl. Acad. Sci. U.S.A.*, **99**, 4459–4464.
  33. Wang,H., Shao,Z., Shi,L.Z., Hwang,P.Y., Truong,L.N., Berns,M.W., Chen,D.J. and Wu,X. (2012) CtIP protein dimerization is critical for its recruitment to chromosomal DNA double-stranded breaks. *J. Biol. Chem.*, **287**, 21471–21480.
  34. Lin,Y.H., Yuan,J., Pei,H., Liu,T., Ann,D.K. and Lou,Z. (2015) KAP1 Deacetylation by SIRT1 Promotes Non-Homologous End-Joining Repair. *PLoS One*, **10**, e0123935.
  35. Temviriyankul,P., van Hees-Stuivenberg,S., Delbos,F., Jacobs,H., de Wind,N. and Jansen,J.G. (2012) Temporally distinct translesion synthesis pathways for ultraviolet light-induced photoproducts in the mammalian genome. *DNA Repair*, **11**, 550–558.
  36. Schlacher,K., Wu,H. and Jasin,M. (2012) A distinct replication fork protection pathway connects Fanconi anemia tumor suppressors to RAD51-BRCA1/2. *Cancer Cell*, **22**, 106–116.
  37. Saleh-Gohari,N., Bryant,H.E., Schultz,N., Parker,K.M., Cassel,T.N. and Helleday,T. (2005) Spontaneous homologous recombination is induced by collapsed replication forks that are caused by endogenous DNA single-strand breaks. *Mol. Cell Biol.*, **25**, 7158–7169.
  38. Bekker-Jensen,S., Lukas,C., Kitagawa,R., Melander,F., Kastan,M.B., Bartek,J. and Lukas,J. (2006) Spatial organization of the mammalian genome surveillance machinery in response to DNA strand breaks. *J. Cell Biol.*, **173**, 195–206.
  39. Leonhardt,H., Rahn,H.P., Weinzierl,P., Sporbert,A., Cremer,T., Zink,D. and Cardoso,M.C. (2000) Dynamics of DNA replication factories in living cells. *J. Cell Biol.*, **149**, 271–280.
  40. Davis,A.J., Chi,L., So,S., Lee,K.J., Mori,E., Fattah,K., Yang,J. and Chen,D.J. (2014) BRCA1 modulates the autophosphorylation status of DNA-PKcs in S phase of the cell cycle. *Nucleic Acids Res.*, **42**, 11487–11501.
  41. Pickering,A., Panneerselvam,J., Zhang,J., Zheng,J., Zhang,Y. and Fei,P. (2013) In vitro FANCD2 monoubiquitination by HHR6 and hRad18. *Cell Cycle*, **12**, 3448–3449.
  42. Garcia-Higuera,I., Taniguchi,T., Ganesan,S., Meyn,M.S., Timmers,C., Hejna,J., Grompe,M. and D'Andrea,A.D. (2001) Interaction of the Fanconi anemia proteins and BRCA1 in a common pathway. *Mol. Cell*, **7**, 249–262.
  43. Taniguchi,T., Garcia-Higuera,I., Andreassen,P.R., Gregory,R.C., Grompe,M. and D'Andrea,A.D. (2002) S-phase-specific interaction of the Fanconi anemia protein, FANCD2, with BRCA1 and RAD51. *Blood*, **100**, 2414–2420.
  44. Nakanishi,K., Yang,Y.G., Pierce,A.J., Taniguchi,T., Digweed,M., D'Andrea,A.D., Wang,Z.Q. and Jasin,M. (2005) Human Fanconi anemia monoubiquitination pathway promotes homologous DNA repair. *Proc. Natl. Acad. Sci. U.S.A.*, **102**, 1110–1115.
  45. Yan,Z., Guo,R., Paramasivam,M., Shen,W., Ling,C., Fox,D. 3rd, Wang,Y., Oostra,A.B., Kuehl,J., Lee,D.Y. *et al.* (2012) A ubiquitin-binding protein, FAAP20, links RNF8-mediated ubiquitination to the Fanconi anemia DNA repair network. *Mol. Cell*, **47**, 61–75.
  46. Sims,A.E., Spiteri,E., Sims,R.J. 3rd, Arita,A.G., Lach,F.P., Landers,T., Wurm,M., Freund,M., Neveling,K., Hanenberg,H. *et al.* (2007) FANCI is a second monoubiquitinated member of the Fanconi anemia pathway. *Nat. Struct. Mol. Biol.*, **14**, 564–567.
  47. Kim,H. and D'Andrea,A.D. (2012) Regulation of DNA cross-link repair by the Fanconi anemia/BRCA pathway. *Genes Dev.*, **26**, 1393–1408.
  48. Hashimoto,Y., Ray Chaudhuri,A., Lopes,M. and Costanzo,V. (2010) Rad51 protects nascent DNA from Mre11-dependent degradation and promotes continuous DNA synthesis. *Nat. Struct. Mol. Biol.*, **17**, 1305–1311.
  49. Schlacher,K., Christ,N., Siaud,N., Egashira,A., Wu,H. and Jasin,M. (2011) Double-strand break repair-independent role for BRCA2 in blocking stalled replication fork degradation by MRE11. *Cell*, **145**, 529–542.
  50. Raderschall,E., Bazarov,A., Cao,J., Lurz,R., Smith,A., Mann,W., Ropers,H.H., Sedivy,J.M., Golub,E.I., Fritz,E. *et al.* (2002) Formation of higher-order nuclear Rad51 structures is functionally linked to p21 expression and protection from DNA damage-induced apoptosis. *J. Cell Sci.*, **115**, 153–164.
  51. Lehmann,A.R. (2006) New functions for Y family polymerases. *Mol. Cell*, **24**, 493–495.
  52. Kuang,L., Kou,H., Xie,Z., Zhou,Y., Feng,X., Wang,L. and Wang,Z. (2013) A non-catalytic function of Rev1 in translesion DNA synthesis and mutagenesis is mediated by its stable interaction with Rad5. *DNA Repair*, **12**, 27–37.
  53. Pages,V., Bresson,A., Acharya,N., Prakash,S., Fuchs,R.P. and Prakash,L. (2008) Requirement of Rad5 for DNA polymerase zeta-dependent translesion synthesis in *Saccharomyces cerevisiae*. *Genetics*, **180**, 73–82.
  54. Moldovan,G.L. and D'Andrea,A.D. (2009) How the fanconi anemia pathway guards the genome. *Annu. Rev. Genet.*, **43**, 223–249.
  55. Nakanishi,K., Cavallo,F., Perrouault,L., Giovannangeli,C., Moynahan,M.E., Barchi,M., Brunet,E. and Jasin,M. (2011) Homology-directed Fanconi anemia pathway cross-link repair is dependent on DNA replication. *Nat. Struct. Mol. Biol.*, **18**, 500–503.
  56. McIlwraith,M.J., Vaisman,A., Liu,Y., Fanning,E., Woodgate,R. and West,S.C. (2005) Human DNA polymerase eta promotes DNA synthesis from strand invasion intermediates of homologous recombination. *Mol. Cell*, **20**, 783–792.